Avrupa Bilim ve Teknoloji Dergisi
Özel Sayı 34, S. 28-33, Mart 2022

Araştırma Makalesi

www.ejosat.com ISSN:2148-2683

European Journal of Science and Technology
Special Issue 34, pp. 28-33, March 2022

Research Article

The Effect of Indium Addition on the Corrosion Kinetics of Sn–3Ag–0.5Cu Alloy in HCl Acid Solution

Serkan Oguz[1*], Ahmet Mustafa Erer[2], Yunus Türen[3], Hayrettin Ahlatçı[4]

[1*] Karabük University, Faculty of Science, Departmant of Physics, Karabük, Turkey, (ORCID: 0000-0001-6315-8970), soguz78@gmail.com
[2] Karabük University, Faculty of Science, Departmant of Physics, Karabük, Turkey, (ORCID: 0000-0003-4358-4010), mustafaerer@karabuk.edu.tr
[3] Karabük University, Faculty of Metallurgical and Materials Engineering, Departmant of Engineering, Karabük, Turkey, (ORCID: 0000-0001-8755-1865), yturen@karabuk.edu.tr
[4] Karabük University, Faculty of Metallurgical and Materials Engineering, Departmant of Engineering, Karabük, Turkey, (ORCID: 0000-0002-6766-4974), hahlatci@karabuk.edu.tr

(2nd International Conference on Applied Engineering and Natural Sciences ICAENS 2022, March 10-13, 2022)

(**DOI:** 10.31590/ejosat.1062757)

ATIF/REFERENCE: Oguz, S., Erer, A. M., Türen, Y. & Ahlatçı, H. (2022). The Effect of Indium Addition on the Corrosion Kinetics of Sn–3Ag–0.5Cu Alloy in HCl Acid Solution. *European Journal of Science and Technology*, (34), 28-33.

Abstract

The aim of this study is to investigate the corrosion behavior of potentiodynamic polarization indium added Sn-3Ag-0.5Cu alloy in 1M HCl solution. SEM and EDX analyses were examined the properties of the alloy samples. Polarization analyses showed by the addition of 0.5, 1, and 2 wt.% indium to the SAC305 solder alloy does not lead to notably different corrosion potentials. The pseudo-passivation region is observed instead of a true passivation region that currents are nearly constant. By the scanning interval, this pseudo-passive region does not have a reactivation point. On the other hand, corrosion rates follow a pattern in which 0.5% wt of indium substitution of silver causes the corrosion rate to decrease. However, with further silver replacement by indium, the rate of corrosion increases. According to the results of microstructure analysis, the formation of corrosion products and the existence of voids and porous structures limit their stability.

Keywords: In-addition, corrosion, microstructure, Pb-free solder alloy, HCl.

HCl Asit Çözeltisinde Sn-3Ag-0.5Cu Alaşımının Korozyon Kinetiği Üzerine İndiyum İlavesinin Etkisi

Öz

Bu çalışmanın amacı potansiyodinamik polarizasyon indiyum ilaveli Sn-3Ag-0.5Cu alaşımının 1M HCl çözeltisinde korozyon davranışını araştırmaktır. Alaşım numunelerinin özellikleri SEM ve EDX analizleri ile incelenmiştir. SAC305 lehim alaşımına ağırlıkça % 0,5, 1 ve 2 ağırlıkça indiyum eklenmesiyle gösterilen polarizasyon analizleri, belirgin şekilde farklı korozyon potansiyellerine yol açmaz. Akımların neredeyse sabit olduğu gerçek bir pasivasyon bölgesi yerine yalancı pasifleştirme bölgesi gözlemlenir. Tarama aralığına göre, bu sözde pasif bölge bir yeniden etkinleştirme noktasına sahip değildir. Öte yandan, korozyon hızları, gümüşün ağırlıkça %0.5'lik indiyum ikamesinin korozyon hızının düşmesine neden olduğu bir model izler. Bununla birlikte, gümüşün indiyumla daha fazla değiştirilmesiyle korozyon hızı artar. Mikroyapı analiz sonuçlarına göre korozyon ürünlerinin oluşması ve kararlılıklarına sınırlar getiren boşluk ve gözenekli yapıların varlığını ortaya koyar.

Anahtar Kelimeler: In-ilavesi, korozyon, mikroyapı, kurşunsuz lehim alaşımı, HCl.

[*] Corresponding Author: soguz78@gmail.com

1. Introduction

Soldering technology is one of the most affected areas in science and technology-based industries, especially in electronics, with rapid growth (Jumali, 2018). Undertaking the task of an environment that provides the distribution of the heat produced by the semiconductor conductors, soldering tech- nology is used to provide thermal, electrical, and mechanical continuity in electronic devices (Abtew, 2000). In the electrical and electrical industry, lead-based solder alloys have been used on electronic devices for a long time (Wang, 2015). The widely used solder alloy is Sn-Pb alloy due to its good wettability with copper pad, easy handling, and other advantages (Han, 2020). With the development of alternative lead-free solder alloys within the scope of RoHS and WEEE directives that prohibit the use of lead-based solder in terms of environment and human health, a significant improvement has been achieved in new soldering technology (Jumali, 2018). As an alternative to the traditional Sn-Pb solder alloy, the new lead-free solder alloys should have almost similar properties. Sn-Ag (Kang, 2015), Sn-Cu (Maeshima, 2016), Sn-Bi (Silva,2015), Sn-Zn (Nazeri, 2014), Sn-Zn-Bi (El-Daly, 2009), Sn-Zn-Ag (Luo, 2012), and Sn–Ag–Cu (SAC) (Hah, 2019) such as diverse types of lead-free solder alloys have been developed. The most preferred solder alloy is the SAC family and has been widely used due to its optimized performance in terms of wetting properties (Xu, 2018; Yang, 2016; Yoon, 2009). In ad- dition, it has been found that SAC solder alloys have some disadvantages such as high melting temperature, thick inter- metallic compounds, and this may cause problems in solder joints (Sayyadi, 2018; El-Daly, 2012; Han, 2020). The most important factor with SAC family solder alloys is the formation of undesirable intermetallic compounds (IMCs) such as Ag_3Sn and Cu_6Sn_5. These IMCs layers adversely solder alloys affect corrosion resistance and mechanical properties (Kaushik, 2018).

Considering the mobility of electronic devices, it may be faced with factors such as atmospheric conditions, humidity, properties of the physical environment, chemicals contain- ing hydroxide and chloride. Although many measures have been taken for the corrosion resistance of solder joints under normal operating conditions, full protection from the ag- gressive environment has not always been achieved (Liu, 2015a; Liu, 2015b). Proper product life can be predicted if the corrosion behav- ior of Pb-free solders is properly investigated and under- stood (Nazeri, 2019). Therefore, information about the microstructural changes, morphology, and growth behavior of the layers of IMCs and their effects on corrosion resistance is crucial to understanding the reliability of SAC-based soldering (Kaushik, 2018). Numerous studies have been conducted on the corrosion behavior of SAC305 solder alloy in solutions (such as NaCl solution) (Mohanty, 2008; Rosalbino, 2009; Osorio, 2011). However, Solder alloys commonly used in electronic devices tend to undergo atmospheric corro- sion. In weather conditions such as humidity, rain, and snow, abrasions occur on the solder surface (Zou, 2013; Liao, 2018). During the corrosion of the alloy depending on the environmental change, there may be situations such as the transfer process of the dissolved oxygen amount, the hydrolytic behavior of dissolved metal, and the process of accumulating corrosion products accordingly (Cheng, 2004). For the solder alloy to be con- sidered reliable, it must have excellent corrosion resistance to certain electrolytes. For many metals and alloys, Hy- drochloric acid (HCl) is considered one of the most corrosive solutions (Jumali, 2017). The junction points of solder alloys must exhibit good corrosion behavior when are directly exposed to an aggressive environment in an industrial environment (Azis, 2020).

There is a marked lack of studies on lead-free solder alloys the electrochemical corrosion behavior in hydrochloric acid (HCl) solution. Thus, in this work, the effect of In on corrosion dynamics of Sn–(3-x) Ag–0.5Cu–xIn (where x=0, 0.5, 1, and 2) in 1 M HCl acid solution was investigated. Corrosion tests have been performed in HCl solution by potentiodynamic polarization and scanning electron microscope (SEM) coupled with energy dispersive X-ray analysis (EDX) were used to determine compositions of the corrosion products.

2. Experimental Procedure

We produced in our previous studies were investigated in corrosion properties of new low Ag-containing Sn-(3-x)Ag-0.5Cu-xIn quaternary Pb-free alloys (Erer, 2019), investigated in 1M HCL solution. Microstructure analyzes of SAC305 and SAC-xIn lead-free solder alloys were separately measured before and after corrosion, using the "CARL ZEISS ULTRA PLUS GEMINI FESEM" and "Q150R ROTARY-PUMPED SPUTTER COATER / CARBON COATER" model SEM device. The samples of the working electrodes are polished with SiC papers with mesh size starting with 400 and ending with 1200. The polishing process is completed with an Al_2O_3 microparticle solution on a smooth cloth. Prepared samples are cleaned with alcohol and dried. To provide potentiostatic stabilization of the working electrode surfaces, open circuit monitoring is performed for 10 minutes before the polarization process. An Ag/AgCl reference electrode with a pair of graphite rods is used as the counter electrode, and samples are used as the working electrodes of the normal three-electrode setup. The acid solution, which is a very aggressive and corrosive medium, is used for solder alloy samples (1M HCl). Potentials between -1.0V - Ag/AgCl and +1.0V - Ag/AgCl are scanned to ensure possible passivation and depassivation sites are found. The scanning rate is 1 mV/s (Erer, 2021).

3. Results and Discussion

3.1. Solder Characterization

Fig. 1 represents the microstructures of SAC305 and SAC-xIn (0.5%, 1, and 2 wt%) lead-free solder alloys. In the displayed SEM analysis, the porous structures show the β-Sn matrix showing the Sn-rich area, the Cu_6Sn_5 phase with large particles called Sn-Cu intermetallic, and the small particles Ag_3Sn intermetallic particles. Meanwhile, Ag_3Sn and Cu_6Sn_5 phases dispersed in the β-Sn matrix also appear to contain a complete eutectic structure (El-Taher, 2021; Subri, 2020). Forms up to 2% In solid solution at room temperature. Therefore, secondary phases associated with In do not occur.

In Fig. 2, the XRD analysis results of the samples of the examined lead-free solder alloys. According to the microstructure results, the peaks for all samples are associated with the Sn-rich phase, with the presence of Ag_3Sn and Cu_6Sn_5 intermetallics for Sn-Ag and Sn-Cu alloys, respectively.

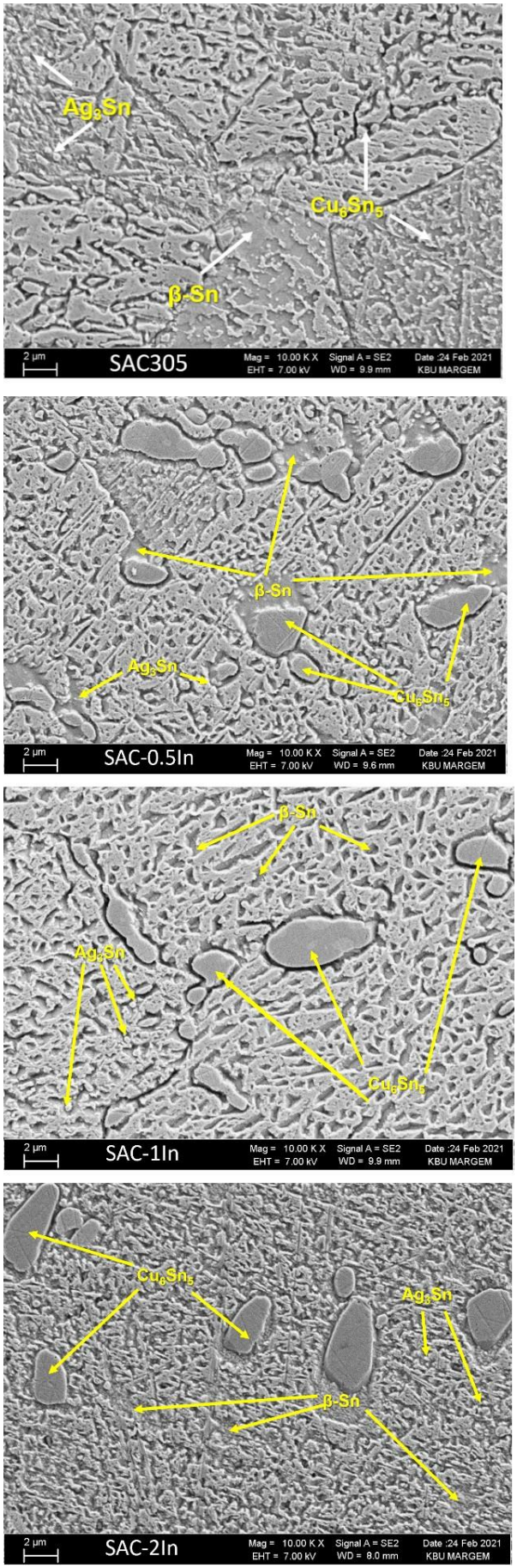

Figure 1: SEM images for the as-prepared SAC305 and SAC- xIn (0.5, 1 and 2 wt. %).

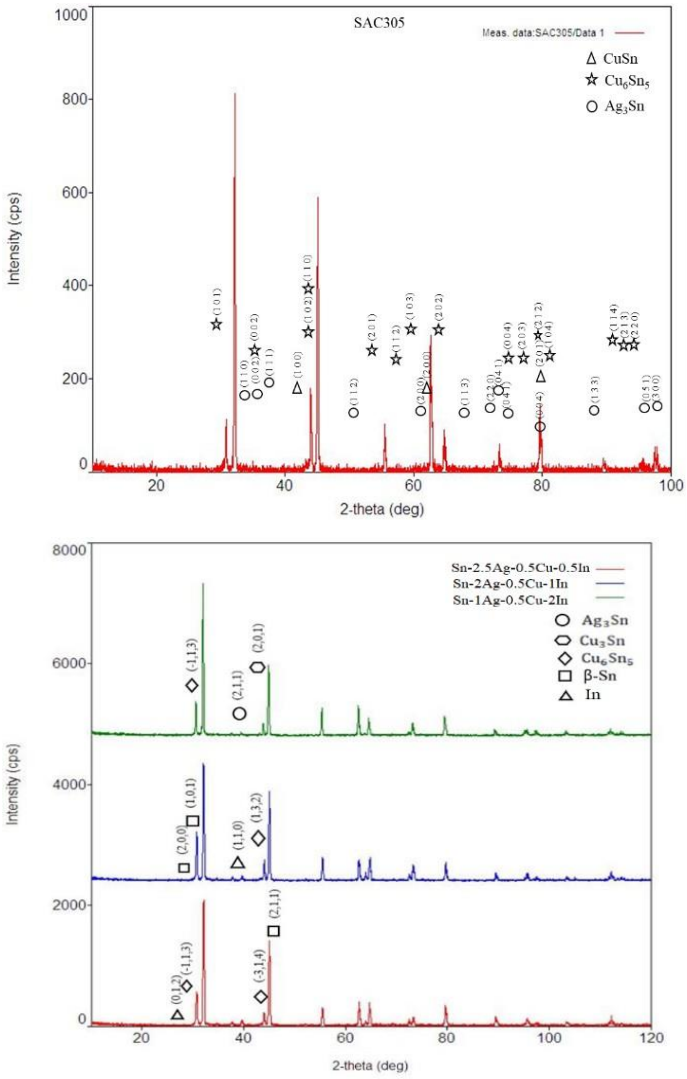

Figure 2: XRD analysis of SAC305 and SAC-xIn (0.5, 1, and 2 wt. %). (Uyanık, 2019).

3.2. Potanciodynamic Polarization Analysis

Plots of potentiodynamic polarization scannings are given in Fig. 3. The absence of passivation regions is clear. In a passivation region, the current density should change its course at some specific potential of anodic polarization and accept very low values compared to values observed just before entering the region. Instead, SAC305 and SAC-xIn (0.5, 1 and 2 wt.%) have only a pseudo-passivation region in which current densities are constant and don't react to changes in scanning potentials from about +0.1 V to the end of the scanning region (+1.0 V). All indium-containing sub-alloys enter this pseudo-passivation region slightly later (with 0.1 V difference) than SAC305. Note that current density in pseudo-passivation regions is much higher than one can have with NaCl solution (Nordin, 2014). This should be expected because of the extreme acidity of the 1M HCl environment. Another interesting point is that of lack of a reactivation point at which the pseudo-passivation region ends. As one can easily see from Fig. 3, even at the end of the scanning region (+1.0 V) pseudo-passivation region holds. This is different from the observed behavior reported by other studies which mainly used NaCl-based solutions (El-Taher, 2021; Subri, 2020). The quantitative results of potentiodynamic po- larization measurements are given in Table 1. We observed similar corrosion potentials for all of the alloys within this study. This is expected

as the ratios of indium within these alloys are not high enough o trigger a significant change. Using Tafel extrapolations, we obtain corrosion current den- sities with corresponding corrosion rates of each alloy. It seems that the whole corrosion rates follow a type with the 1.0% indium substitution of silver causing the corrosion rate to decrease. However, with further replacement of silver by indium, the rate of corrosion increases.

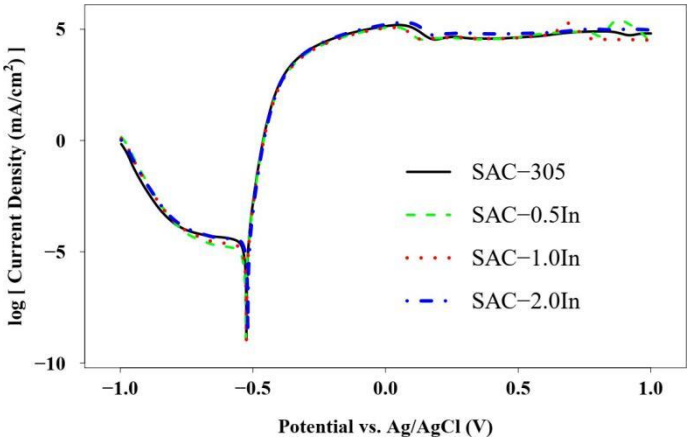

Figure 3: Potentiodynamic polarization curves of SAC305 and SAC-xIn (0.5, 1 and 2 wt. %).).

A low Corrosion Current Density (i_{corr}) value means hat the corrosion rate is low. The higher the corrosion rate, he higher the corrosion rate. Adding the indium element o the SAC305 solder alloy and reducing the silver element reduces the i_{corr} values. The lowest corrosion rate belongs to SAC-0.5In, and the highest corrosion rate belongs to SAC305 solder alloy. In this case, the rate of corrosion was reduced by replacing 0.5% indium element with silver. It is seen that the rate of corrosion increases as the ratio of indium element is replaced by silver at 1% and 2% ratios. However, the results show that the corrosion rate is reduced compared to the SAC305 solder alloy. When the corrosion rate is examined, it can be said that the SAC-0.5In alloy, which has the lowest rate, is more resistant to corrosion than the SAC305 alloy.

Table 1. Corrosion parameters of SAC305 and SAC-xIn (0.5, 1 and 2 wt. %).

Specimen	i_{corr} ($\mu A/cm^2$)	CR (mm/year)	E_{corr} (V)
SAC-0.5In	9.246	0.249	-0.529
SAC-1In	10.571	0.285	-0.528
SAC-2In	15.730	0.424	-0.520
SAC305	18.095	0.488	-0.525

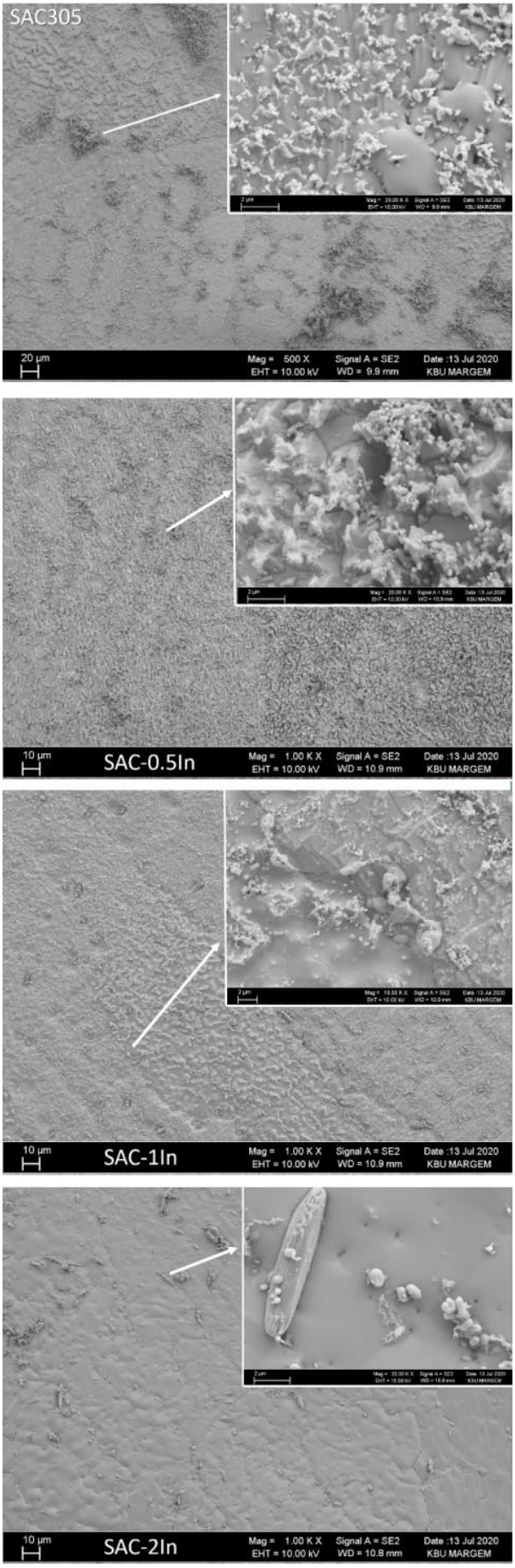

Figure 4: SEM surface morphologies of SAC305 and SAC-xIn (0.5, 1, and 2 wt. %) solder alloys after immersion in 1M HCl solution.

3.3. Post-Corrosion Characterizations

In Fig. 4, the views of the analyzed lead-free solder alloys after the potentiodynamic tests are given. It is seen that the oxide film formed as a corrosion product with the increase of "In" addition to the SAC305 solder alloy gradually coarsens and becomes coarse spherical at the addition of 2% In. As can be seen from the EDX analysis of corrosion products, it has been observed that corrosion products have Ag content by weight up to 0.5% wt In addition, and larger spherical Cu-containing regions increase with the addition of more.

4. Conclusions and Recommendations

In this study, the corrosion behavior of SAC305 and SAC-xIn (0.5 wt%, 1 and 2 wt%) lead-free solder alloys was investigated under the influence of 1 M HCl (pH =0). Similar E_{corr} and i_{corr} were found for all alloys. This is to be expected as the proportions of indium in these alloys are not high enough to trigger a significant change. As a result of the examination, the overall corrosion rates follow a situation where the 0.5% indium replacement of silver causes the corrosion rate to decrease significantly. However, the corrosion rate appears to increase with the greater displacement of silver by indium. However, the corrosion rate increases with the further displacement of silver by indium.

References

Abtew, M., & Selvaduray, G. (2000). Lead-free Solders in Microelectronics. *Materials Science and Engineering: R: Reports*, *27*(5-6), 95-141. https://doi.org/10.1016/S0927-796X(00)00010-3

Aziz, M. Z. H., Zainon, N., Mohamad, A. A., & Nazeri, M. F. M. (2020). Corrosion Investigation of Sn-0.7Cu Pb-Free Solder in Open-Circuit and Polarized Conditions. *IOP Conference Series: Materials Science and Engineering*, *957*, 012012. https://doi.org/10.1088/1757-899X/957/1/012012

Cheng, Y. L., Zhang, Z., Cao, F. H., Li, J. F., Zhang, J. Q., Wang, J. M., & Cao, C. N. (2004). A study of the corrosion of aluminum alloy 2024-T3 under thin electrolyte layers. *Corrosion Science*, *46*(7), 1649-1667. https://doi.org/10.1016/j.corsci.2003.10.005

El-Daly, A. A., & Hammad, A. E. (2012). Enhancement of creep resistance and thermal behavior of eutectic Sn–Cu lead-free solder alloy by Ag and In-additions. *Materials & Design*, *40*, 292-298. https://doi.org/10.1016/j.matdes.2012.04.007

El-Daly, A. A., Swilem, Y., Makled, M. H., El-Shaarawy, M. G., & Abdraboh, A. M. (2009). Thermal and mechanical properties of Sn–Zn–Bi lead-free solder alloys. *Journal of Alloys and Compounds*, *484*(1-2), 134-142. https://doi.org/10.1016/j.jallcom.2009.04.108

El-Taher, A. M., & Razzk, A. F. (2021). Controlling Ag3Sn Plate Formation and Its Effect on the Creep Resistance of Sn–3.0Ag–0.7Cu Lead-Free Solder by Adding Minor Alloying Elements Fe, Co, Te and Bi. *Metals and Materials International*, *27*(10), 4294-4305. https://doi.org/10.1007/s12540-020-00856-w

Erer, A. M., & Uyanik, O. (2019). Influence of Indium Content on the Wetting Behaviours of Sn-(3-x)Ag-0.5Cu-xIn Alloy Systems. *Acta Physica Polonica A*. https://doi.org/10.12963/APhysPolA.135.766

Erer, A.M. (2021). Effect of bismuth addition on the corrosion dynamics of Sn-3Ag-0.5Cu solder alloy in Hydrochloric Acid Solution. *International Journal of Innovative Engineering Applications*, 5 (1), 40-44. https://doi.org/10.46460/ijiea.911862

Hah, J., Kim, Y., Fernandez-Zelaia, P., Hwang, S., Lee, S., Christie, L., Houston, P., Melkote, S., Moon, K.-S., & Wong, C.-P. (2019). Comprehensive comparative analysis of microstructure of Sn–Ag–Cu (SAC) solder joints by traditional reflow and thermo-compression bonding (TCB) processes. *Materialia*, *6*, 100327. https://doi.org/10.1016/j.mtla.2019.100327

Han, Y. D., Gao, Y., Jing, H. Y., Wei, J., Zhao, L., & Xu, L. Y. (2020). A modified constitutive model of Ag nanoparticle-modified graphene/Sn–Ag–Cu/Cu solder joints. *Materials Science and Engineering: A*, *777*, 139080. https://doi.org/10.1016/j.msea.2020.139080

Jumali, N., Mohamad, A. A., & Mohd Nazeri, M. F. (2017). Corrosion Properties of Sn-9Zn Solder in Acidic Solution. *Materials Science Forum*, *888*, 365-372. https://doi.org/10.4028/www.scientific.net/MSF.888.365

Jumali, N., Zainol, M. H., Mohamad, A. A., & Nazeri, M. F. M. (t.y.). *Effect of Al Additions on Corrosion Performance of Sn-9Zn Solder in Acidic Solution*. *273*, 5.

Kang, H., Lee, M., Sun, D., Pae, S., & Park, J. (2015). Formation of octahedral corrosion products in Sn–Ag flip chip solder bump. *Scripta Materialia*, *108*, 126-129. https://doi.org/10.1016/j.scriptamat.2015.06.034

Kaushik, R. K., Batra, U., & Sharma, J. D. (2018). Aging induced structural and electrochemical corrosion behaviour of Sn-1.0Ag-0.5Cu and Sn-3.8Ag-0.7Cu solder alloys. *Journal of Alloys and Compounds*, *745*, 446-454. https://doi.org/10.1016/j.jallcom.2018.01.292

Liao, B., Cen, H., Chen, Z., & Guo, X. (2018). Corrosion behavior of Sn-3.0Ag-0.5Cu alloy under chlorine-containing thin electrolyte layers. *Corrosion Science*, *143*, 347-361. https://doi.org/10.1016/j.corsci.2018.08.041

Liu, J.-C., Park, S., Nagao, S., Nogi, M., Koga, H., Ma, J.-S., Zhang, G., & Suganuma, K. (2015a). The role of Zn precipitates and Cl− anions in pitting corrosion of Sn–Zn solder alloys. *Corrosion Science*, *92*, 263-271. https://doi.org/10.1016/j.corsci.2014.12.014

Liu, J.-C., Zhang, G., Ma, J.-S., & Suganuma, K. (2015b). Ti addition to enhance corrosion resistance of Sn–Zn solder alloy by tailoring microstructure. *Journal of Alloys and Compounds*, *644*, 113-118. https://doi.org/10.1016/j.jallcom.2015.04.168

Luo, T., Chen, Z., Hu, A., & Li, M. (2012). Study on melt properties, microstructure, tensile properties of low Ag content Sn–Ag–Zn Lead-free solders. *Materials Science and Engineering: A*, *556*, 885-890. https://doi.org/10.1016/j.msea.2012.07.086

Maeshima, T., Ikehata, H., Terui, K., & Sakamoto, Y. (2016). Effect of Ni to the Cu substrate on the interfacial reaction with Sn-Cu solder. *Materials & Design*, *103*, 106-113. https://doi.org/10.1016/j.matdes.2016.04.068

Mohanty, U. S., & Lin, K.-L. (2008). Electrochemical corrosion behaviour of Pb-free Sn–8.5Zn–0.05Al–XGa and Sn–3Ag–0.5Cu alloys in chloride containing aqueous solution. *Corrosion Science*, *50*(9), 2437-2443. https://doi.org/10.1016/j.corsci.2008.06.042

Mohd Nazeri, M. F., Yahaya, M. Z., Gursel, A., Cheani, F., Masri, M. N., & Mohamad, A. A. (2019). Corrosion characterization of Sn-Zn solder: A review. *Soldering & Surface Mount*

Technology, *31*(1), 52-67. https://doi.org/10.1108/SSMT-05-2018-0013

Nazeri, M. F. M., & Mohamad, A. A. (2014). Corrosion measurement of Sn–Zn lead-free solders in 6 M KOH solution. *Measurement*, *47*, 820-826. https://doi.org/10.1016/j.measurement.2013.10.002

Nordin, N. I. M., Said, S. M., Ramli, R., Sabri, M. F. M., Sharif, N. M., Arifin, N. A. F. N. M., & Ibrahim, N. N. S. (2014). Microstructure of Sn–1Ag–0.5Cu solder alloy bearing Fe under salt spray test. *Microelectronics Reliability*, *54*(9-10), 2044-2047. https://doi.org/10.1016/j.microrel.2014.07.068

Osório, W. R., Spinelli, J. E., Afonso, C. R. M., Peixoto, L. C., & Garcia, A. (2011). Microstructure, corrosion behaviour and microhardness of a directionally solidified Sn–Cu solder alloy. *Electrochimica Acta*, *56*(24), 8891-8899. https://doi.org/10.1016/j.electacta.2011.07.114

Rosalbino, F., Angelini, E., Zanicchi, G., Carlini, R., & Marazza, R. (2009). Electrochemical corrosion study of Sn–3Ag–3Cu solder alloy in NaCl solution. *Electrochimica Acta*, *54*(28), 7231-7235. https://doi.org/10.1016/j.electacta.2009.07.030

Sayyadi, R., & Naffakh-Moosavy, H. (2018). Physical and mechanical properties of synthesized low Ag/lead-free Sn-Ag-Cu-xBi (x = 0, 1, 2.5, 5 wt%) solders. *Materials Science and Engineering: A*, *735*, 367-377. https://doi.org/10.1016/j.msea.2018.08.071

Silva, B. L., Reinhart, G., Nguyen-Thi, H., Mangelinck-Noël, N., Garcia, A., & Spinelli, J. E. (2015). Microstructural development and mechanical properties of a near-eutectic directionally solidified Sn–Bi solder alloy. *Materials Characterization*, *107*, 43-53. https://doi.org/10.1016/j.matchar.2015.06.026

Subri, N. W. B., Sarraf, M., Nasiri-Tabrizi, B., Ali, B., Mohd Sabri, M. F., Basirun, W. J., & Sukiman, N. L. (2020). Corrosion insight of iron and bismuth added Sn–1Ag–0.5Cu lead-free solder alloy. *Corrosion Engineering, Science and Technology*, *55*(1), 35-47. https://doi.org/10.1080/1478422X.2019.1666458

Uyanık, O., Erer, A. M., & Türen, Y. (2019). Effect of Indium on Wettability of Sn-2Ag-0,5Cu-1In Quaternary Solder Alloy on Cu Substrate. *El-Cezeri Fen ve Mühendislik Dergisi*. https://doi.org/10.31202/ecjse.441434

Wang, H., Gao, Z., Liu, Y., Li, C., Ma, Z., & Yu, L. (2015). Evaluation of cooling rate on electrochemical behavior of Sn–0.3Ag–0.9Zn solder alloy in 3.5 wt% NaCl solution. *Journal of Materials Science: Materials in Electronics*, *26*(1), 11-22. https://doi.org/10.1007/s10854-014-2356-6

Xu, L. Y., Zhang, S. T., Jing, H. Y., Wang, L. X., Wei, J., Kong, X. C., & Han, Y. D. (2018). Indentation Size Effect on Ag Nanoparticle-Modified Graphene/Sn-Ag-Cu Solders. *Journal of Electronic Materials*, *47*(1), 612-619. https://doi.org/10.1007/s11664-017-5822-0

Yang, M., Ji, H., Wang, S., Ko, Y.-H., Lee, C.-W., Wu, J., & Li, M. (2016). Effects of Ag content on the interfacial reactions between liquid Sn–Ag–Cu solders and Cu substrates during soldering. *Journal of Alloys and Compounds*, *679*, 18-25. https://doi.org/10.1016/j.jallcom.2016.03.177

Yoon, J.-W., Noh, B.-I., Kim, B.-K., Shur, C.-C., & Jung, S.-B. (2009). Wettability and interfacial reactions of Sn–Ag–Cu/Cu and Sn–Ag–Ni/Cu solder joints. *Journal of Alloys and Compounds*, *486*(1-2), 142-147. https://doi.org/10.1016/j.jallcom.2009.06.159

Zou, S., Li, X., Dong, C., Ding, K., & Xiao, K. (2013). Electrochemical migration, whisker formation, and corrosion behavior of printed circuit board under wet H2S environment. *Electrochimica Acta*, *114*, 363-371. https://doi.org/10.1016/j.electacta.2013.10.051